

# Anderson-Bogoliubov collective excitations in superfluid Fermi gases at nonzero temperatures

S. N. Klimin · H. Kurkjian · J. Tempere

November 10, 2021

**Abstract** The Anderson-Bogoliubov branch of collective excitations in a condensed Fermi gas is treated using the effective bosonic action of Gaussian pair fluctuations. The spectra of collective excitations are treated for finite temperature and momentum throughout the BCS-BEC crossover. The obtained spectra explain, both qualitatively and quantitatively, recent experimental results on Goldstone modes in atomic Fermi superfluids.

**Keywords** Ultracold Fermi gases · Collective excitations · Anderson-Bogoliubov mode

## 1 Introduction

The Anderson-Bogoliubov (AB) collective excitations (also named Goldstone modes in the low-momentum limit) are sound-like oscillations of a superfluid phase of condensed Bose or Fermi gases. They are already widely studied theoretically both at  $T = 0$  and at nonzero temperatures. Sound modes in superconductors were first considered by Anderson [1] within the random phase approximation. Spectra of AB collective excitations for ultracold atomic gases in the zero-temperature case have been well established within the Gaussian pair fluctuation theory (GPF) and the RPA, both in the long-wavelength limit [1, 2, 3, 4, 5] and for nonzero phonon momentum [6, 7], and within the fermion-boson model [8]. For nonzero temperatures in the  $q \rightarrow 0$

limit, the sound velocity [9, 10, 11] and damping [13, 14, 15, 16, 17, 18] were predicted theoretically, and partially measured [19]. The damping of collective modes by a particle-hole continuum was recently observed in the normal phase of Helium-3 [20]. Previous theoretical approaches are limited to the low temperature regime, where the spectrum can be calculated perturbatively from the zero temperature case. The present work is focused on the energy spectrum and the damping factor of AB modes in ultracold Fermi gases in the whole BCS-BEC crossover range with finite momentum at nonzero temperature. The treatment is based on the GPF effective action, which incorporates the effect of one-phonon absorption/emission by a fermionic quasiparticle in the collective mode spectrum. Other effects, e. g., three- and four-phonon scattering processes [15] are beyond the scope of the present work. The obtained spectra of AB collective excitations are verified by comparison with recent experimental results [19], both in the long-wavelength limit and at a nonzero phonon momentum. We also discuss the relation of the present approach and obtained results to preceding works on AB collective excitations.

## 2 Collective oscillation excitations in a superfluid Fermi gas

We consider collective excitations on a superfluid Fermi gas on the basis of the partition function which is the path integral on the bosonic pairing field  $(\bar{\Psi}, \Psi)$

$$\mathcal{Z} \propto \int \mathcal{D} [\bar{\Psi}, \Psi] e^{-S_{\text{eff}}}, \quad (1)$$

---

S. N. Klimin · H. Kurkjian · J. Tempere  
TQC, Universiteit Antwerpen, Universiteitsplein 1, B-2610  
Antwerpen, Belgium  
E-mail: jacques.tempere@uantwerpen.be

J. Tempere  
Lyman Laboratory of Physics, Harvard University, Cam-  
bridge, Massachusetts 02138, USA

with the effective bosonic action  $S_{\text{eff}}$ ,

$$S_{\text{eff}} = - \int_0^\beta d\tau \int d\mathbf{r} \frac{1}{g} \bar{\Psi}(\mathbf{r}, \tau) \Psi(\mathbf{r}, \tau) - \text{Tr} \ln [-\mathbb{G}^{-1}], \quad (2)$$

where  $\beta$  is inverse to temperature, and  $g$  is the coupling constant for the contact fermion-fermion interaction, which is renormalized through the  $s$ -wave scattering length  $a_s$  as in Ref. [5]. Throughout the paper, the units are  $\hbar = 1$ , the fermion mass  $m = 1/2$ , and the Fermi wave vector  $k_F = (3\pi^2 n)^{1/3} = 1$ ,  $n$  being the particle density. The bosonic partition function for an interacting Fermi gas appears as a result of the Hubbard-Stratonovich transformation [5]. In this effective action,  $\mathbb{G}^{-1}(\mathbf{r}, \tau)$  is the inverse Nambu tensor,

$$\mathbb{G}^{-1}(\mathbf{r}, \tau) = \begin{pmatrix} -\frac{\partial}{\partial \tau} + \nabla_{\mathbf{r}}^2 + \mu & \Psi(\mathbf{r}, \tau) \\ \bar{\Psi}(\mathbf{r}, \tau) & -\frac{\partial}{\partial \tau} - \nabla_{\mathbf{r}}^2 - \mu \end{pmatrix}, \quad (3)$$

with the chemical potential  $\mu$ .

The partition function is determined within this model by Eq. (1) with the action (2). Next, we consider collective excitations which are oscillation modes of the pairing field about a uniform saddle-point value  $\Psi(\mathbf{r}, \tau) = \Delta$ :

$$\Psi(\mathbf{r}, \tau) = \Delta + \varphi(\mathbf{r}, \tau), \quad \bar{\Psi}(\mathbf{r}, \tau) = \Delta + \bar{\varphi}(\mathbf{r}, \tau) \quad (4)$$

where  $\Delta$  is determined by the least action principle and satisfies the saddle-point gap equation,

$$\int \frac{d\mathbf{k}}{(2\pi)^3} \left( \frac{\tanh\left(\frac{\beta E_{\mathbf{k}}}{2}\right)}{2E_{\mathbf{k}}} - \frac{1}{2k^2} \right) + \frac{1}{8\pi a_s} = 0, \quad (5)$$

where  $E_{\mathbf{k}} = \sqrt{\xi_{\mathbf{k}}^2 + \Delta^2}$  is the Bogoliubov excitation energy with the free-particle energy  $\xi_{\mathbf{k}} = k^2 - \mu$ .

For the analysis of small oscillations about the least action solution, we keep the quadratic expansion of the effective bosonic action. The quadratic Gaussian pair fluctuation (GPF) action in the Matsubara  $(\mathbf{q}, i\Omega_n)$  representation is the  $(2 \times 2)$  matrix:

$$S^{(quad)} = \frac{1}{2} \sum_{\mathbf{q}, n} \begin{pmatrix} \bar{\varphi}_{\mathbf{q}, n} & \varphi_{-\mathbf{q}, -n} \end{pmatrix} \times \mathbb{M}(\mathbf{q}, i\Omega_n) \begin{pmatrix} \varphi_{\mathbf{q}, n} \\ \bar{\varphi}_{-\mathbf{q}, -n} \end{pmatrix}, \quad (6)$$

where  $\mathbb{M}(\mathbf{q}, i\Omega_n)$  is the inverse fluctuation propagator [5]. The explicit expressions for matrix elements  $M_{j,k}(q, i\Omega_n)$  used in the present work can be found in Ref. [17].

The expansion (4) with (5) is not enough to determine the gap  $\Delta$  at fixed density and scattering length.

The gap and chemical potentials in the mean-field approximation represent a joint solution of the gap and number mean-field number equations. In general, beyond the mean-field approximation both the gap equation and the equation of state should be modified. However, when the temperature is not very close to  $T_c$ , the equation of state beyond the mean-field approximation, e. g., accounting for Gaussian fluctuations, combined with the mean-field gap equation gives a good quantitative agreement with the Monte Carlo results, except close to the transition temperature [21]. Consequently, we can apply saddle-point gap equation (5) in combination with non-mean-field equations of state what seems to be appropriate for the experimental condition  $T \approx 0.5T_c$  of Ref. [19].

### 3 Spectra of collective excitations

Spectra of collective excitations are approximately revealed using the spectral response function for the system described by the GPF effective action. The spectral response function is determined in the same way as in Ref. [22]:

$$\chi(q, \omega) = \frac{1}{\pi} \text{Im} \frac{M_{1,1}(q, \omega + i0^+)}{\det \mathbb{M}(q, \omega + i0^+)}. \quad (7)$$

In Fig. 1, the shape of the spectral response function is compared with two sets of the experimental results on the sound velocity for AB modes: the raw data for nonzero  $q \approx 0.5k_F$ , shown in the upper panel and the data for a small  $q \rightarrow 0$ , obtained in Ref. [19] using a nonzero-momentum correction and shown in the lower panel. The small-momentum spectral response function in Fig. 1 (b) has been calculated for  $q = 0.01k_F$ , that is sufficiently small for the comparison with the experimental data obtained using the nonzero-momentum correction. In the limit of small  $q$ , the frequency  $\omega_q$  of the AB mode tends to the sound wave dispersion law  $\omega_q \rightarrow v_s q + O(q^3)$  with the AB mode sound velocity  $v_s$ . Consequently, we plot the spectral response function in the variables  $1/a_s$  and  $\omega/(v_F q)$  (where  $v_F$  is the Fermi velocity) in order to visualize sound velocities for the comparison with the experiment.

The spectral response function has been calculated using an interpolation of the Monte Carlo data for the zero-temperature equation of state [23], assuming that  $\mu$  slowly varies in the range of temperatures corresponding to the experiment ( $T \approx 0.5T_c$ ). The gap function has been calculated using the nonzero-temperature gap equation (5) with that chemical potential and with the same values of the temperature as in Ref. [19].

For a nonzero momentum, the ratio  $\omega_q/(v_F q)$  is smaller than  $v_s$  at the BCS side, because the AB mode

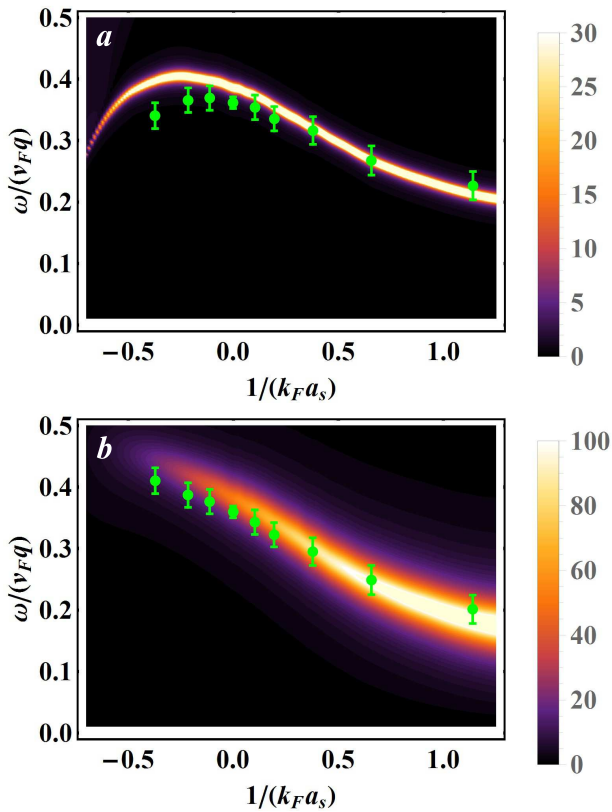


**Fig. 1** (Color online) Scaled spectral response function  $q^2 \chi(q, \omega)$  (a) for finite momentum  $q$  as indicated in Supplement to Ref. [19], (b) for a small  $q = 0.01 k_F$ . Full dots show the experimental data of Ref. [19].

frequency is a concave function of  $q$ . In the BEC case,  $\omega_q$  is convex, and hence  $\omega_q/(v_F q) > v_s$  [7]. The concavity in the BCS regime is well expressed in the figure showing a fast decrease of the raw data of Ref. [19] for the sound velocity when moving to the BCS side in Fig. 1 (a). Correspondingly, the same trend is seen for the maximum of the spectral response function. The sound velocity calculated in Ref. [19] using the nonzero-momentum correction monotonically increases when varying the inverse scattering length from BEC to the BCS regime. However, at fixed  $T$ , there exists a critical value of  $1/a_s$  when  $T = T_c$  [in the far BCS limit, not shown on Fig. 1 (b)]. When approaching this value the sound velocity drops to zero. The AB modes in this range of the inverse scattering length hardly can be resolved experimentally due to an increasing inverse quality factor when approaching the superfluid phase transition [24].

The maximum positions of the spectral response function in Fig. 1 plotted using the scaled variable  $\omega_q/(v_F q)$  lie rather close to the sound velocities measured in the experiment [19]. For definite conclusions, the collective excitation spectra must be determined

explicitly. To properly interpret the broadened peak of the response function in terms of a collective excitation, one should look for the complex root of the equation  $\det \mathbb{M}(q, z) = 0$  [22, 24] where the real and imaginary part of  $z$  are, respectively, the eigenfrequency and damping factor of the AB mode. However, this equation has a priori no root in the complex  $z$  plane. To reveal a root one should perform an analytic continuation of the function  $z \rightarrow \det \mathbb{M}(q, z)$  through its branch cut at the real axis as proposed by Nozières [25] for complex poles of Green's functions. This prescription is performed for matrix elements  $M_{j,k}(q, z)$  of the inverse fluctuation propagator using the spectral function, determined at the real axis:

$$\rho_{j,k}(q, \omega) = \lim_{\delta \rightarrow +0} \frac{M_{j,k}(q, \omega + i\delta) - M_{j,k}(q, \omega - i\delta)}{2i\pi}. \quad (8)$$

This spectral function is (in general, piecewise) analytic on the real axis. It can be thus analytically extended  $[\rho_{j,k}(q, \omega) \rightarrow \rho_{j,k}(q, z)]$  to complex  $z$  with  $\text{Re}(z) = \omega$  and  $\text{Im}(z) < 0$  from each interval where  $\rho_{j,k}(q, \omega)$  is analytic. The analytic continuation of the matrix elements, denoted as  $M_{j,k}^{(R)}(q, z)$ , is then:

$$M_{j,k}^{(R)}(q, z) = \begin{cases} M_{j,k}(q, z), & \text{Im } z > 0, \\ M_{j,k}(q, z) + 2i\pi \rho_{j,k}(z), & \text{Im } z < 0. \end{cases} \quad (9)$$

The equation

$$\det \mathbb{M}^{(R)}(q, z) = 0 \quad (10)$$

has complex roots in the area where  $\text{Im}(z) < 0$ . These roots are denoted as  $z_q = \omega_q - i\Gamma_q/2$ , where  $\omega_q$  is the collective excitation frequency, and  $\Gamma_q$  is the damping factor. The analytic continuation method gives us frequencies and damping factors self-consistently, i. e. accounting for their mutual feedback, so that the damping factor is obtained beyond the frequently used perturbation approach (see for discussion Refs. [9, 16, 22]).

The momentum dependence of the frequencies and damping factors of the AB modes obtained from the equation (10) is shown in Fig. 2 for two cases relevant for the experiment [19]: in the BCS regime with  $1/a_s = -0.6$  and at unitarity,  $1/a_s = 0$ . Like above, the background parameters ( $\mu, \Delta$ ) are found from the Monte Carlo equation of state and the finite-temperature gap equation (5). The momentum dependence of the AB mode frequency is qualitatively the same as in preceding works [7, 9, 10], but quantitatively differs from them because we use different background parameters, and we include the nonzero temperature energy shift. The AB mode energy tends to the pair-breaking threshold energy for considered values of momentum when increasing  $q$ . The damping factor exhibits a maximum at

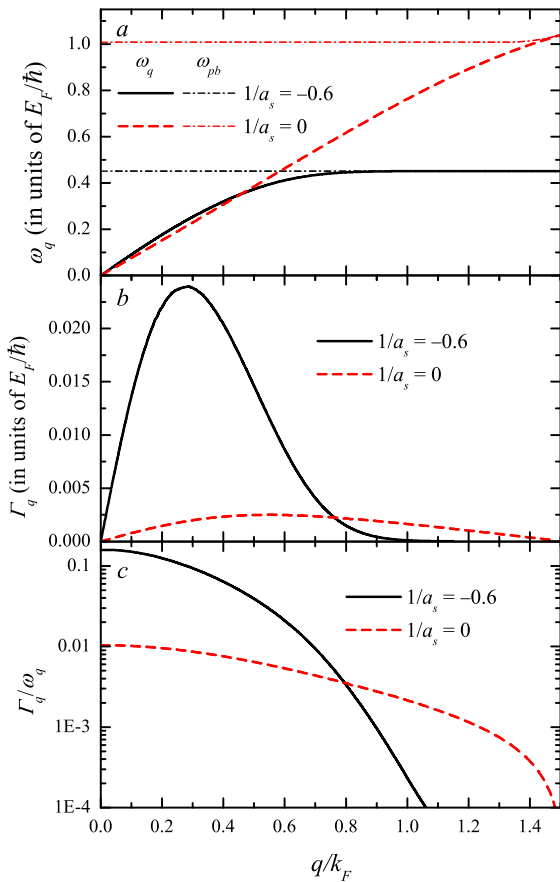


**Fig. 2** (Color online) (a) Frequencies of AB modes of a superfluid Fermi gas as a function of momentum for  $1/a_s = -0.6$  (solid curve) and for  $1/a_s = 0$  (dashed curve). Dot-dashed curves: the pair breaking threshold frequencies. (b) The damping factor and (c) the inverse quality factor for the same inverse scattering lengths as in the panel (a).

nonzero  $q$  and diminishes when the excitation energy approaches the pair-breaking threshold. The momentum dependence of the inverse quality factor  $\Gamma_q/\omega_q$  for AB modes is similar to that obtained in Ref. [16] (where the AB mode spectra were determined using mean-field background parameters and within a perturbative approximation).

When approaching the pair-breaking continuum, the terms of  $M_{j,k}(q, z)$  which describe the breaking of a pair into fermionic quasiparticles (terms with denominators  $z \pm (E_{\mathbf{k}} + E_{\mathbf{k}+\mathbf{q}})$ , see [16]) become almost resonant and repel the AB branch, forbidding it to enter the continuum. Since the branch stays outside the continuum, these terms are never exactly resonant and so, never contribute to the damping rate. Still, they render the terms describing absorption-emission processes [with denominators  $z \pm (E_{\mathbf{k}} - E_{\mathbf{k}+\mathbf{q}})$ ] negligible, what explains the suppression of the absorption-emission damping rate on Fig. 2 when approaching the pair-breaking continuum.

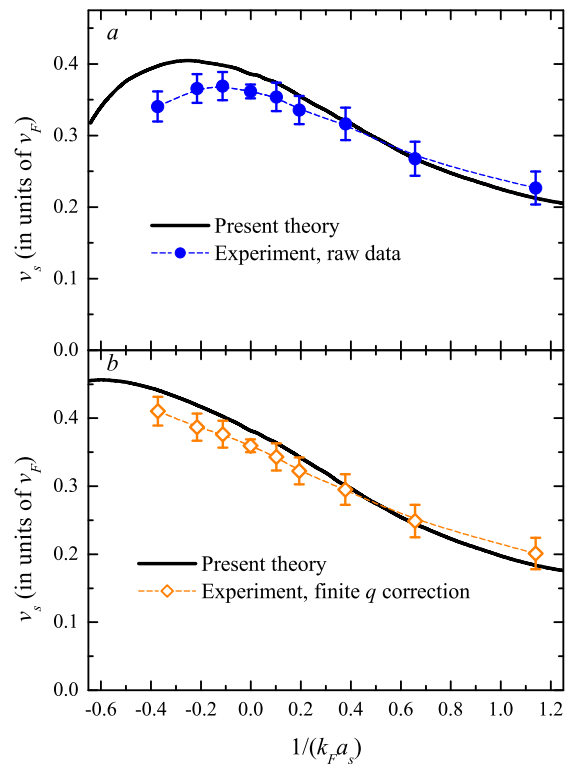


**Fig. 3** (Color online) (a) Scaled AB mode frequencies  $\omega_q/(v_F q)$  obtained from the equation for the collective excitations with finite  $q$  determined in Ref. [19]. The symbols show the experimental results of Ref. [19]. (b) The same with  $q = 0.01k_F$  used in our calculation, compared with the finite  $q$  correction result of the experiment.

The comparison of sound velocities obtained using the analytic continuation of the inverse fluctuation propagator with the experimental data of Ref. [19] is shown in Fig. 3. As can be seen from Fig. 3, the calculated sound velocities are in good agreement with the experiment [19]. A difference between the calculated and measured sound velocities can be attributed to several reasons: an inaccuracy of the experimental determination of input parameters (e. g., the temperature and the momentum), a difference of the chemical potential from its precise nonzero-temperature values, and possibly an influence of induced interactions, which can be significant in the BCS regime [26].

## 4 Conclusions

In the present work, we analyze spectra and damping factors for nonzero-momentum AB collective excitations in superfluid Fermi gases as a function of the temperature, momentum and the interaction strength. The treatment is based on the effective Gaussian pair fluctuation action for the pairing field. This approach

is well substantiated when anharmonicity effects can be neglected.

The energy spectrum of AB modes has been qualitatively shown using the pairing field spectral response function. Then, quantitative results for the AB mode spectra have been obtained from complex roots of the analytically continued determinant of the inverse fluctuation propagator. This method provides a self-consistent non-perturbative solution for the AB mode frequency and the damping factor.

The experimental sound velocity is compared in Ref. [19] with several theoretical predictions [5, 27, 28, 29]. In order to clarify the novelty of the present work, it is worth noting that they concern the sound velocity obtained in the precise  $q \rightarrow 0$  limit at  $T = 0$ , while the present work is focused at the  $q \neq 0$  behavior of AB modes at a nonzero temperature, what is more appropriate for a comparison with the experiment. The existing theory of AB modes for  $q \neq 0$ , e. g., [6, 7] exploits the mean-field equation of state, what also favors the relevance of the present study, where more realistic equations of state are used.

The AB mode spectra have been calculated using reliable background parameters obtained accounting for fluctuations. As a result, calculated sound velocities of AB modes exhibit a good agreement with experimental data.

**Acknowledgements** The present work is supported by the University Research Fund (BOF) of the University of Antwerp and by the Flemish Research Foundation (FWO-VI), project No. G.0429.15.N and the European Union's Horizon 2020 research and innovation program under the Marie Skłodowska-Curie grant agreement No. 665501.

## References

1. P. W. Anderson, "Random-Phase Approximation in the Theory of Superconductivity", Phys. Rev. **112**, 1900 (1958).
2. J. R. Engelbrecht, M. Randeria, and C. A. R. Sá de Melo, "BCS to Bose crossover: Broken-symmetry state", Phys. Rev. B **55**, 15153 (1997).
3. M. Marini, F. Pistolesi, and G.C. Strinati, "Evolution from BCS superconductivity to Bose condensation: analytic results for the crossover in three dimensions", Eur. Phys. J. B **1**, 151 (1998).
4. L. Salasnich, "Goldstone and Higgs Hydrodynamics in the BCS-BEC Crossover", Condens. Matter **2**, 22 (2017).
5. R. B. Diener, R. Sensarma, and M. Randeria, "Quantum fluctuations in the superfluid state of the BCS-BEC crossover", Phys. Rev. A **77**, 023626 (2008).
6. R. Combescot, M. Yu. Kagan, and S. Stringari, "Collective mode of homogeneous superfluid Fermi gases in the BEC-BCS crossover", Phys. Rev. A **74**, 042717 (2006).
7. H. Kurkjian, Y. Castin, and A. Sinatra, "Concavity of the collective excitation branch of a Fermi gas in the BEC-BCS crossover", Phys. Rev. A **93**, 013623 (2016).
8. B. Huang and S. Wan, "Collective modes in a uniform Fermi gas with Feshbach resonances", Phys. Rev. A **75**, 053608 (2007).
9. Y. Ohashi and A. Griffin, "Superfluidity and collective modes in a uniform gas of Fermi atoms with a Feshbach resonance", Phys. Rev. A **67**, 063612 (2003).
10. P. Pieri, L. Pisani, and G. C. Strinati, "BCS-BEC crossover at finite temperature in the broken-symmetry phase", Phys. Rev. B **70**, 094508 (2004).
11. I. Kosztin, Q. Chen, Y.-J. Kao, and K. Levin, "Pair excitations, collective modes, and gauge invariance in the BCS - Bose-Einstein crossover scenario", Phys. Rev. B **61**, 11662 (2000).
12. W. V. Liu, "Effective Theory of Excitations in a Feshbach-Resonant Superfluid", Phys. Rev. Lett. **96**, 080401 (2006).
13. Z. Zhang and W. V. Liu, "Finite-temperature damping of collective modes of a BCS-BEC crossover superfluid", Phys. Rev. A **83**, 023617 (2011).
14. P. Zou, H. Hu, and X.-J. Liu, "Low-momentum dynamic structure factor of a strongly interacting Fermi gas at finite temperature: The Goldstone phonon and its Landau damping", arXiv:1712.08318.
15. H. Kurkjian, Y. Castin and A. Sinatra, "Three-Phonon and Four-Phonon Interaction Processes in a Pair-Condensed Fermi Gas", Ann. Phys. **529**, 1600352 (2017).
16. H. Kurkjian and J. Tempere, "Absorption and emission of a collective excitation by a fermionic quasiparticle in a Fermi superfluid", New J. Phys. **19**, 113045 (2017).
17. S. N. Klimin, J. Tempere, and J. P. A. Devreese, "Pair Excitations and Parameters of State of Imbalanced Fermi Gases at Finite Temperatures", J. Low. Temp. Phys. **165**, 261 (2011).
18. Y. Castin, A. Sinatra, and H. Kurkjian, Phys. Rev. Lett. **119**, 260402 (2017).
19. S. Hoinka, P. Dyke, M. G. Lingham, J. J. Kinnunen, G. M. Bruun, and C. J. Vale, "Goldstone mode and pair-breaking excitations in atomic Fermi superfluids", Nat. Phys. **13**, 943 (2017); arXiv:1707.00406.
20. H. Godfrin, M. Meschke, H.-J. Lauter, A. Sultan, H. M. Böhm, E. Krotscheck and M. Panholzer, "Observation of a roton collective mode in a two-dimensional Fermi liquid", Nature **483**, 576 (2012).
21. H. Hu, X.-J. Liu and P. D. Drummond, "Equation of state of a superfluid Fermi gas in the BCS-BEC crossover", Europhys. Lett., **74**, 574 (2006).
22. H. Kurkjian, S. N. Klimin, J. Tempere, and Y. Castin, "Collective branch in the continuum of BCS superconductors and superfluid Fermi gases", arXiv:1805.02462.
23. G. E. Astrakharchik, J. Boronat, J. Casulleras, and S. Giorgini, "Equation of State of a Fermi Gas in the BEC-BCS Crossover: A Quantum Monte Carlo Study", Phys. Rev. Lett. **93**, 200404 (2004).
24. S. N. Klimin, H. Kurkjian and J. Tempere, "Sound velocity and damping in superfluid Fermi gases at nonzero temperatures", arXiv:1811.07796.
25. Philippe Nozières, "Le problème à N corps: propriétés générales des gaz de fermions" (Dunod, Paris, 1963).
26. L. P. Gor'kov and T. K. Melik-Barkhudarov, "Contribution to the Theory of Superfluidity in an Imperfect Fermi Gas", Sov. Phys. JETP **13**, 1018 (1961).
27. N. Manini and L. Salasnich, "Bulk and collective properties of a dilute Fermi gas in the BCS-BEC crossover", Phys. Rev. A **71**, 033625 (2005).

- 
28. R. Haussmann, W. Rantner, S. Cerrito, and W. Zwerger, “*Thermodynamics of the BCS-BEC crossover*”, Phys. Rev. A **75**, 023610 (2007).
  29. H. Tajima, P. van Wyk, R. Hanai, D. Kagamihara, D. Inotani, M. Horikoshi, and Y. Ohashi, “*Strong-coupling corrections to ground-state properties of a superfluid Fermi gas*”, Phys. Rev. A **95**, 043625 (2017).